Electronic Supplementary Material (ESI) for Journal of Materials Chemistry C.

Seed Mediated Copper Nanoparticle Synthesis for Fabricating Oxidation Free Interdigitated Electrodes using Intense Pulse Light Sintering for Flexible Printed Chemical Sensors

Krishnamraju Ankireddy,[†] Thad Druffel,[†] Swathi Vunnam,[‡] Gregor Filipič,[†□] Ruvini Dharmadasa,[℗] Delaina A. Amos[¥*]

[†] Conn Center for Renewable Energy Research, University of Louisville, Louisville, KY-40292, USA
[¥]Department of Chemical Engineering, University of Louisville, Louisville, KY 40292
[‡] Department of Mechanical Engineering, University of Louisville, Louisville, KY-40292, USA
[□] Jozef Stefan Institute, Jamova cesta 39, 1000 Ljubljana, Slovenia, EU
[℗] Bert Thin Films, LLC. 201 E. Jefferson St., Louisville, KY-40202, USA
***Corresponding Author**
(D.A)Email: delaina.amos@louisville.edu

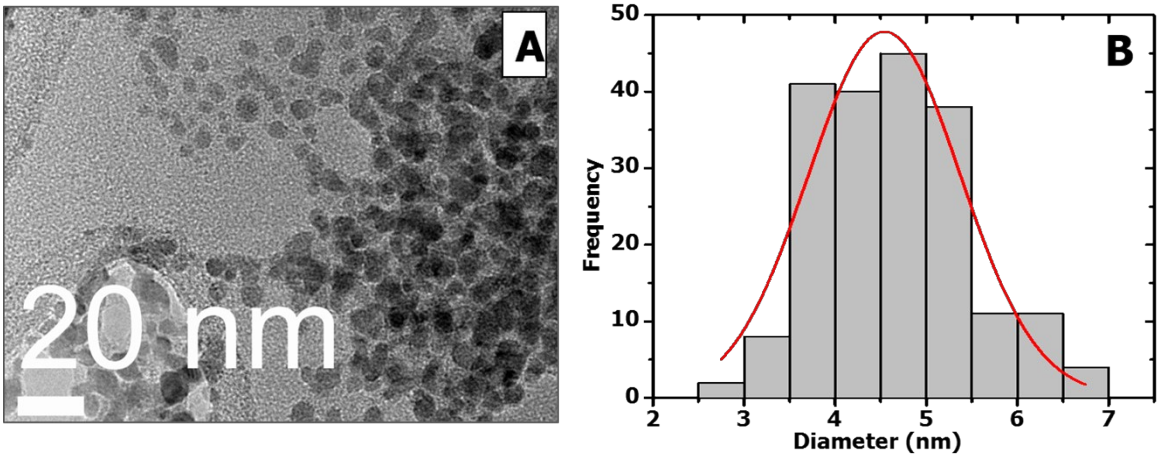

Figure S1. Structural characterization of seed copper nanoparticles: (A) TEM image of the seed particles, (B) Particle size distribution.

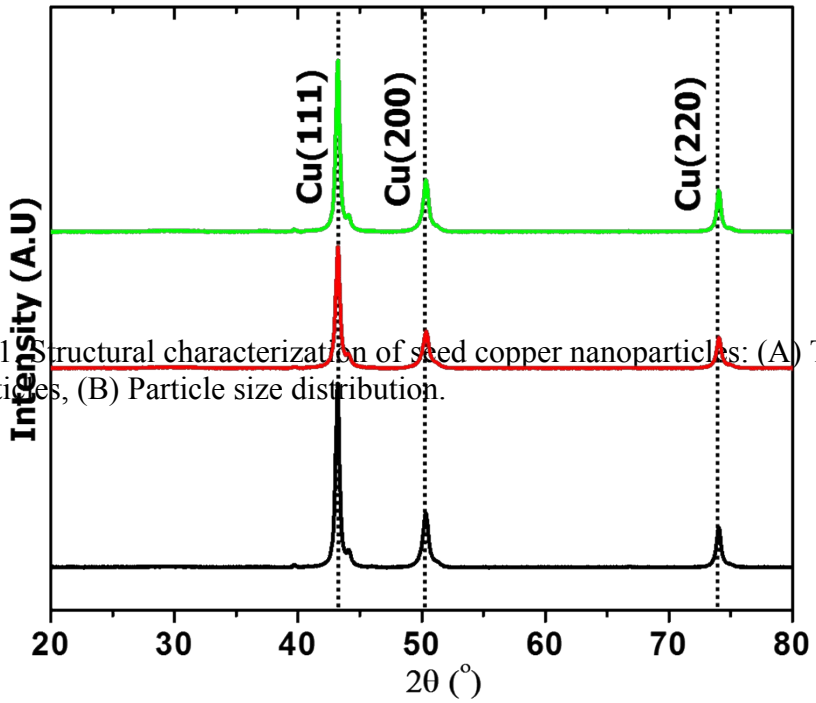

Figure S2. XRD spectra of seed mediated copper nanoparticles from three separate batches of syntheses.

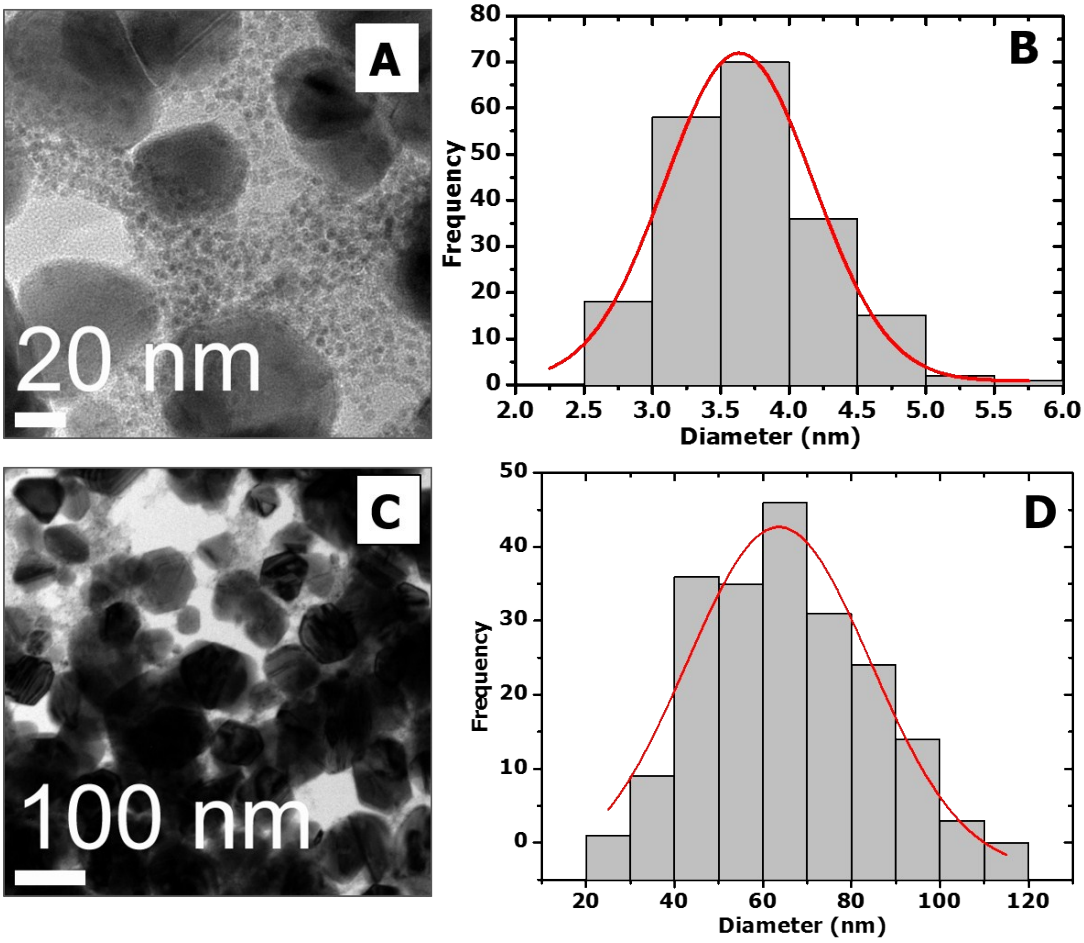

Figure S3. Structural characterization of seed mediated copper nanoparticles: (A) Magnified TEM image to show smaller size particles, (B) the size distribution of the smaller size particles, (C) Lower magnification image to show the bigger size particles , and (D) the size distribution of the bigger size particles.

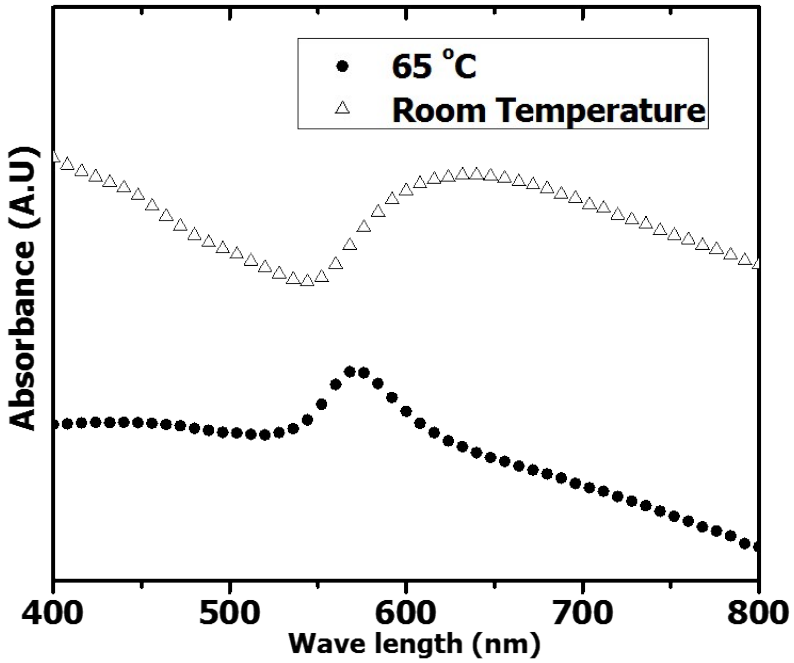

Figure S4. UV-Visible analysis of the seed mediated growth particles synthesized at room temperature and 65 °C.

Energy Density (J/cm^2)	Number of Pulses	Resistance (Ω)
12.4	1	3
17.2	1	1.7
19	1	1.3
20.1	1	0.7
23.3	1	1.7
25	1	1.7
27.6	1	1
20.1	2	1.8
20.1	3	1.4
20.1	4	3.8
20.1	5	21

Table S1. The change in the resistance of a copper pattern with different IPL input conditions.

Printed Pattern Resistance under Bending

we conducted experiments on the printed line by bending/wrapping around tubes of different radius. The table below shows the resistance increase with decrease in the bend radius and the figure shows the experimental set up for the bend test.

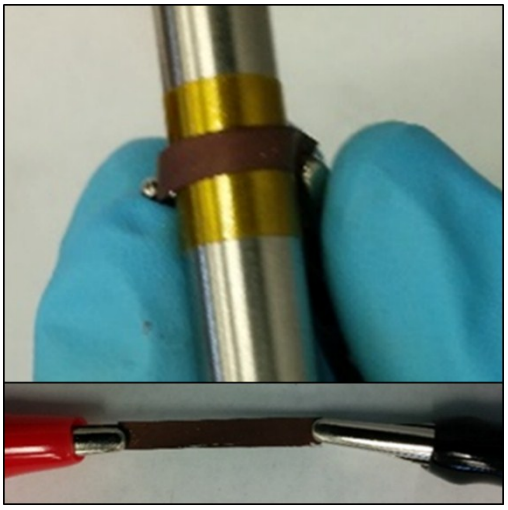

Figure S5: Printed pattern under bending and no-bending

Bend Radius (mm)	Resistance (Ω)	% Increase After Bending
0	1.3	0.0
7	1.3	0.0
6	1.7	30.8
5	2	53.8
3	2.6	100.0

Table S2: The increase in the resistance of 25 x 3 mm printed pattern with decrease in the bend radius.

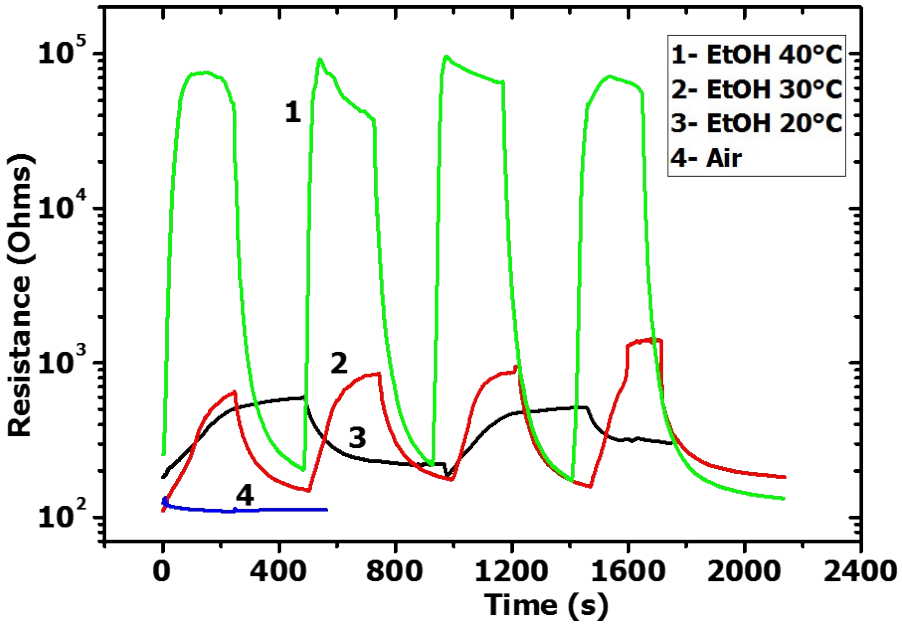

Figure S6. Resistance change with ethanol vapor concentration at different temperatures. The resistance of the sensor was constant (4-Air) when it was suspended in the empty flask kept on a hot plate temperature of 60 C .

Sensor Bending Tests

We conducted sensing experiments again on the same sensor that was used for sensor results in the manuscript approximately three months apart. Since the sensor was exposed to atmospheric conditions during this interval, the response of the unbent sensor has reduced. This time, the sensing was conducted with bending/wrapping the sensor around different tube radii of 6 mm and 1.5 mm. The response under bending was improved comparing to unbent sensor, even as much as 4000 %. This could be due to more widening of the gaps or micro-cracks between the graphite flakes in the PEG matrix under bending and allowing more ethanol vapor to be absorbed by the polymer. The table S3 shows the response of the sensor under bending.

Bending Radius (mm)	Increase in Response (%)
No Bending	0
6	3865
1.5	3458

Table S3. The change in the response after bending at different radii comparing to unbent sensor.

Sensitivity of the sensor

Sensitivity is a change of measured signal per analyte concentration unit, i.e., the slope of a calibration graph [1] and *the detection limit* is the lowest concentration of the analyte that can be

detected by the sensor under given conditions, particularly at a given temperature. [2] In our case however, we have shown a *proof of concept device* with the ethanol sensor, and we performed the sensing measurements at rather high concentrations and evaluated the sensitivity which was not linear and it was roughly between 0.01 and 1 % per ppm. Compared to the literature, these values are not so high (i.e. 510 % per ppm [10] or 100 % per ppm [5]); however, in contrast to the majority of sensors that need to be heated to work, our sensor is operational also at room temperature and its sensitivity is comparable to that of similar sensors (0.05 % per ppm [3] or 10 % per ppm with the addition of monochromatic light [6]). Since the majority of authors do not report the sensitivity, we took the liberty to estimate the sensitivities from their reported calibration (response) curves as shown in the table and references below.

SnO_2 doped with Co	Metal-oxide resistive sensor	Ambient temperature	0.05 %/ppm	[3]
SnO_2 nanorods with NiO nanparticles	Metal-oxide resistive sensor	300 °C	4.8 %/ppm Non-linear response	[4]
ZnO nanowires on the optical fiber surface	Metal-oxide resistive sensor	300 °C under UV light	100 %/ppm	[5]
Bi_2S_3 sensor between transparent FTO electrodes	Surface photovoltage (SPV) measurement	Room temperature under monochromatic light	10 %/ppm Non-linear response, smaller for larger concentrations	[6]
TiO_2 nanotubes/porous Si heterojunction	Metal-oxide resistive sensor	150 °C	Reported sensitivity 9.3 %/ppm	[7]
ZnO NP doped with Mn	Metal-oxide resistive sensor	240 °C	60 %/ppm	[8]
Cu_2O NP film	Metal-oxide resistive sensor	240 °C	Non-linear response 1.8 %/ppm (small concentrations) 0.3 %/ppm (larger concentrations)	[9]
Sm_2O_3 loaded flower-like ZnO	Metal-oxide resistive sensor	300 °C	510 %/ppm	[10]

nanostructures				

Table S4. Sensitivity of Chemical sensors

IPL Sintering with L-Absorbic Acid and other ligands as capping agents for copper nanoparticles

The L-ascorbic acid is mainly used in this study to cap the particles from oxidation and can be removed relatively easily from the surface of the nanoparticles during post processing of the printed patterns to become electrically conductive. The L-ascorbic acid is physically adsorbed on the surface without forming any strong chemical bonds with the surface atoms of the copper nanoparticles. To our knowledge, the sintering mechanism of L-ascorbic acid capped nanoparticles with IPL processing has not been reported previously. However, our XRD results show that the particles are effectively capped with L-ascorbic acid so that there is no oxidation of as-synthesized particles and using only one pulse yielded conductive patterns. This effective removal of L-ascorbic acid with 20.1 J/cm^2 in one pulse indicates that the IPL process and L-ascorbic acid have a good synergy. However, we did not further explore to quantify the L-ascorbic acid content before and after the IPL process.

We compared our results with those from literature in terms of the IPL energy and number of pulses utilized to sinter PVP and other binder-capped copper nanoparticles. The table below summarizes some of the IPL sintering work on the copper nanoparticles. The energy density, number of pulses, and pulse duration were reported in the range of 12-60 J/cm^2, 1-8 pulses, and 2-10 ms pulse duration, respectively. In our study, we used IPL input settings (20.1J/cm^2, 1pulse, and 2 ms duration) at the lower end of this range and still achieved resistivity comparable to previous studies.

Literature	**Ink Formulation**	**IPL Conditions**	**Resistivity/Resistance**
Kim et al [11]	Commericial Cu Nps	50 J/cm^2, 2 ms pulse	5 μΩ·cm
Ryu et al [12]	PVP capped Cu Nps	50 J/cm^2, 2 ms pulse	5.2 μΩ·cm
Wang et al [13]	Cu ion ink	40-60 J/cm^2 , 20 to 46 pulses	3.21−5.27 μΩ·cm
Han et al [14]	PVP capped Cu nps	32 J/cm^2, 8 pulses	173 μΩ.cm
Chung et al [15]	Precursor and Cu nps hybrid ink	12 J/cm^2 , 10 ms pulse	27.3 μΩ cm
Hwang et al [16]	PVP capped Cu nps	12.5 J/cm^2, 10 ms pulse	72 mΩ/sq

Table S5. Resistivity for IPL sintered copper nanoparticles with different capping agents

References

[1] Ahmad Umar and Yoon-Bong Hahn. *Metal oxide nanostructures and their applications*, volume 5. American Scientific Publ., 2010.

[2] Alankar Shrivastava and Vipin Gupta. Methods for the determination of limit of detection and limit of quantitation of the analytical methods. *Chronicles of Young Scientists*, 2(1):21–21, 2011.

[3] M Parthibavarman, B Renganathan, and D Sastikumar. Development of high sensitivity ethanol gas sensor based on co-doped SnO_2 nanoparticles by microwave irradiation technique. *Current Applied Physics*, 13(7):1537–1544, 2013.

[4] Gun-Joo Sun, Jae Kyung Lee, Wan In Lee, Ram Prakash Dwivedi, Chongmu Lee, and Taegyung Ko. Ethanol sensing properties and dominant sensing mechanism of nio-decorated SnO_2 nanorod sensors. *Electronic Materials Letters*, 13(3):260–269, 2017.

[5] Bo Gong, Tielin Shi, Wei Zhu, Guanglan Liao, Xiaoping Li, Jie Huang, Tengyuan Zhou, and Zirong Tang. Uv irradiation-assisted ethanol detection operated by the gas sensor based on zno nanowires/optical fiber hybrid structure. *Sensors and Actuators B: Chemical*, 245:821–827, 2017.

[6] Xiaoyun Yang, Shasha Tian, Rui Li, Wan Wang, and Shaomin Zhou. Use of single-crystalline Bi_2S_3 nanowires as room temperature ethanol sensor synthesized by hydrothermal approach. *Sensors and Actuators B: Chemical*, 241:210–216, 2017.

[7] Priyanka Dwivedi, Neha Chauhan, P Vivekanandan, Samaresh Das, D Sakthi Kumar, and Saakshi Dhanekar. Scalable fabrication of prototype sensor for selective and sub-ppm level ethanol sensing based on TiO_2 nanotubes decorated porous silicon. *Sensors and Actuators B: Chemical*, 249:602–610, 2017.

[8] Jinxiao Wang, Jun Yang, Ning Han, Xinyuan Zhou, Shuyan Gong, Jianfeng Yang, Peng Hu, and Yunfa Chen. Highly sensitive and selective ethanol and acetone gas sensors based on modified zno nanomaterials. *Materials & Design*, 121:69–76, 2017.

[9] Ahmad Sabirin Zoolfakar, Muhammad Zamharir Ahmad, Rozina Abdul Rani, Jian Zhen Ou, Sivacarendran Balendhran, Serge Zhuiykov, Kay Latham, Wojtek Wlodarski, and Kourosh Kalantar-Zadeh. Nanostructured copper oxides as ethanol vapour sensors. *Sensors and Actuators B: Chemical*, 185:620–627, 2013.

[10] Minoo Bagheri, Naghmeh Faal Hamedani, Ali Reza Mahjoub, Abbas Ali Khodadadi, and Yadollah Mortazavi. Highly sensitive and selective ethanol sensor based on Sm_2O_3-loaded flower-like zno nanostructure. *Sensors and Actuators B: Chemical*, 191:283–290, 2014.

[11] Kim, HS., Dhage, S.R., Shim, DE. et al. Appl. Phys. A (2009) 97: 791. https://doi.org/10.1007/s00339-009-5360-6

[12] Ryu, J., Kim, HS. & Hahn, H.T. Journal of Elec Materi (2011) 40: 42. https://doi.org/10.1007/s11664-010-1384-0

[13] Byung-Yong Wang, Tae-Hee Yoo, Yong-Won Song, Dae-Soon Lim, and Young-Jei Oh, ACS Applied Materials & Interfaces 2013 5 (10), 4113-4119, DOI: 10.1021/am303268k

[14] Won-Suk Han, Jae-Min Hong, Hak-Sung Kim and Yong-Won Song, Nanotechnology, Volume 22, Number 39, 2011, http://iopscience.iop.org/article/10.1088/0957-4484/22/39/395705/meta

[15] Wan-Ho Chung, Hyun-Jun Hwanga, Hak-SungKima, volume 580, Thin Solid Films, 2015, https://doi.org/10.1016/j.tsf.2015.03.004

[16] Hyun-Jun Hwang, Wan-Ho Chung, and Hak-Sung Kim, Nanotechnology, volume 23, number 48, 2012, http://iopscience.iop.org/article/10.1088/0957-4484/23/48/485205/meta